Selective Adsorption of Ag(I) from Electronic Waste Leachate Using Modified Silk Sericin

Sijing Zhang[1]*, Fengjiao Ao[1], Yongping Wang[2], Junxue Zhao[3], Yongliang Ji[1] and Shuangli Chen[1]

[1]*School of Science, Xi'an University of Architecture and Technology, 13 Yanta Road, Xi'an, 710055, China*
[2]*Shaanxi Provincial Academy of Environmental Science, 49 North Changan Road, Xi'an, 710061, China*
[3]*School of Metallurgy Engineering, Xi'an University of Architecture and Technology, 13 Yanta Road, Xi'an, 710055, China*

ABSTRACT: A novel biosorbent was synthesized by grafting bisthiourea (BTU) on a silk sericin (SS) matrix. This biosorbent was denoted as BTU-SS and characterized by Fourier transform infrared spectroscopy (FTIR), zeta potential measurements, elemental analysis, and X-ray photoelectron spectroscopy (XPS). As revealed by the adsorption experiments, both BTU-SS and SS showed low affinity towards coexisting base metallic ions in Ag(I)-Cu(II)-Zn(II)-Ni(II)-Pb(II) electronic waste leachate mixtures, while their adsorption capacities towards Ag(I) reached 30.5 and 10.4 mg·g^{-1} at a pH of 5.0, respectively. BTU-SS showed higher selectivity towards Ag(I) than SS, as revealed by the Ag(I) partition coefficients between the biosorbents and the leachate (16634.6 and 403.3, respectively). As further demonstrated by column experiments, BTU-SS allowed the separation of Ag(I) from an electronic waste leachate. Thermodynamic studies showed that the adsorption of Ag(I) was exothermic and spontaneous, while adsorption kinetic experiments revealed that chemisorption dominated the adsorption process with activation energies of 47.67 and 53.27 kJ·mol^{-1} for BTU-SS and SS, respectively. FTIR and XPS analyses of fresh and Ag(I)-loaded BTU-SS further revealed an adsorption mechanism mainly involving electrostatic and coordination interactions.

KEYWORDS: Electronic waste leachate, modified silk sericin, selective adsorption, silver recovery

1 INTRODUCTION

Sericin, one of the protein components of silk, is usually generated from silkworm [1]. Silk sericin (SS) encircles the fibroin in silk fibers and is generally removed during fiber processing into fabrics. The world annual production of cocoon silk is reported to surpass 1 million tons, from which approximately 50,000 tons of SS are waste discharged without further utilization [2]. A proper utilization of SS would undoubtedly benefit the silk industry while mitigating the noticeable eutrophication of the environment. Fortunately, several approaches have been developed to recover and utilize SS as a useful resource in the fields of polymer materials [3–5], cosmetics [6, 7], and biomedical applications with various purposes [8–11]. SS is reported to possess large amounts of functional groups (e.g., amino, carbonyl and carboxyl) which can play active roles in binding and adsorbing metallic

ions [12], thereby allowing SS to be theoretically used as a biosorbent. However, the utilization of SS as a biosorbent of metallic ions from aqueous solutions has scarcely been studied in the literature. Kwak *et al.* [13] reported that over 70% of a Cr(VI) contaminant could be removed on SS. Chen *et al.* [12] reported on the selective biosorption of SS towards precious metals. Thus, SS exhibited higher selectivity towards Au(III) in a multi-component system and poor selectivity towards Ag(I) in an Ag(I)-Cu(II) binary system.

Compared with traditional pyro- and hydrometallurgy methods, biosorption is well recognized as a promising technology allowing the economical and eco-friendly recovery of precious metals [14]. Currently, the research on biosorption of precious metals is mainly focused on gold and platinum metals [12, 15–17], and most of these efforts only reported adsorption capacities and rarely discussed the selectivity of the biosorbents [12, 18]. Since Ag is the most widely used precious metal and one important component of electronic waste (e-waste) leachates and various industrial effluents, Ag biosorption, particularly Ag selective adsorption, should receive more attention

[19] as a crucial separation and recovery technology. In this sense, we decided to study the selective recovery of Ag on SS and its bisthiourea (BTU)-modified derivative (BTU-SS) from an e-waste leachate containing Ag, Cu, Ni, Pb, and Zn. This e-waste recycling approach allowed the recovery of precious metals by using recycled materials, which is important from the viewpoint of sustainability since it substantially reduces the consumption of virgin materials and energy [20].

Although SS suffers from relatively poor selectivity towards Ag(I) [12], this can be overcome by grafting new functional groups onto the SS matrix. As reported by relevant studies [21–23], adsorbents modified with functional groups containing N and S atoms showed excellent adsorption capacities and selectivity towards precious metals. According to the Pearson's Hard-Soft-Acid-Base (HSAB) principle, Ag(I) is a soft acid and thus the incorporation of soft ligand atoms (e.g., N and S) into the SS matrix would remarkably increase the selectivity towards Ag ions via preferential coordination of Ag(I) with the lone pair electrons of N and S atoms. In the present study, the SS matrix was first crosslinked with epichlorohydrin on its active amino groups, and BTU functional groups containing N and S were subsequently introduced on the surface of the crosslinked matrix by chemical modification. Thus, the modified BTU-SS biosorbent was provided with selective adsorption characteristics towards Ag.

This work examined the behavior of SS and BTU-SS during the adsorption of Ag(I) from aqueous solutions. The adsorption thermodynamic parameters were calculated to evaluate the thermodynamic feasibility and spontaneity of the adsorption process, and the adsorption kinetics and biosorption mechanisms on BTU-SS were also investigated. A continuous column test was also carried out to evaluate the suitability of BTU-SS for the selective recovery of Ag(I) from an e-waste leachate.

2 EXPERIMENTAL

All the chemical reagents used in the experiments were analytical grade (Sinopharm Chemical Reagent Shaanxi Co. Ltd.) and used without further purification. Silk worm was kindly donated by a local farmer and the e-waste used for the preparation of the leachate was obtained from a local waste recycling station. Silver nitrate was used for the single Ag(I) adsorption experiments and 0.01 M HCl was used to titrate the amino end-groups on SS with methyl red (0.4 g·L^{-1}) as an indicator. Diluted nitric acid and sodium hydroxide solutions were added to adjust the pH of the solutions. Other reagents used in the experiments included epichlorohydrin, methanol, sodium carbonate, 2,5-dithiourea, and N,N-dimethylformamide.

2.1 SS Extraction and Modification

The SS used in this study was extracted from washed clean silk worm with a 2% sodium carbonate solution at a liquor ratio of 40:1. The solution was heated to boil for 1 h, the residues filtered, and the filtrate collected. The procedure was repeated to boil the residue, and the resultant filtrate was mixed with that previously collected. The filtrate was condensed and desiccated in a convection oven at 338 K for 24 h. Finally, the dried SS product was crushed and stored for further use. Sericin contains both random coil and less-soluble β-sheet structures, with the former being transformed into the latter upon heating and cooling processes [24]. The solubility of the extracted SS in water decreased progressively upon repeated boilings, and this was undoubtedly beneficial for the adsorption process.

As reported by Chen *et al.* [12], SS is rich in alkyl, carboxyl, carbonyl, and amino groups. However, in the absence of an amino-protecting group, ligands are likely to be immobilized on the amino groups via crosslinking because of the higher reactivity of these functionalities as compared to the rest of functional groups generated on SS upon the modification process. Scheme 1 illustrates the possible routes for the modification of SS via grafting of BTU functional groups in the presence of an epichlorohydrin crosslinker. The details of this process are provided below.

First, 4.0 g of SS powder were loaded into a 100 mL three-necked round-bottom flask and 60 mL of
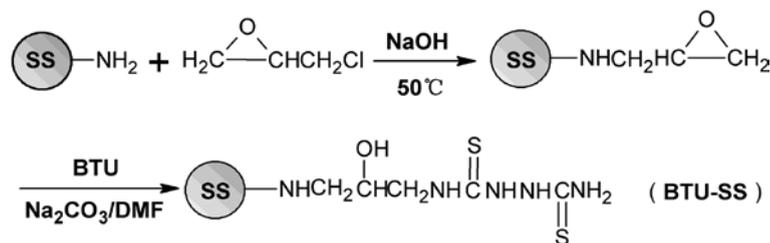
Scheme 1 Synthesis route for BTU-SS. Proposed structure of BTU-SS is depicted, where SS stands for the matrix of silk sericin.

deionized water were subsequently added to allow swelling for 2 h. The pH was adjusted to 11.0 with a 0.10 M NaOH solution and the resultant solution was heated to 323 K. Then, 10.0 mL of epichlorohydrin were slowly added to initiate reaction. The mixture was maintained under continuous stirring for 12 h, and the solid was filtrated and washed first with methanol (to remove the excess epichlorohydrin) and then washed with deionized water until the filtrate became neutral. The solid was dried in a convection oven overnight at 333 K to yield the intermediate; then 2.4 g of the intermediate were loaded into a three-necked flask, and 0.6 g of Na_2CO_3, 1.4 g of BTU powder, and 30 mL of dimethylformamide (DMF) were separately added and the mixture heated to 333 K under continuous stirring for 10 h. The resulting BTU-SS product was filtered, successively washed with deionized water until neutral pH of the filtrate, and dried in a convection oven at 333 K for 24 h. Finally, the dried product BTU-SS was crushed and stored in a bottle for further use.

2.2 Characterization of the Biosorbents

The chemical properties of the biosorbents were characterized by Fourier transform infrared spectroscopy (FTIR, Shimadzu IRPrestige-21, KBr disk technique). For convenience, the spectra of the samples were displayed in the transmittance mode. The surface charge was measured on a zeta potentiometer (Malvern ZEN1590) by using eight SS suspensions with varying pH values (1.0–8.0). Each SS suspension was prepared by dispersing 50 mg of the powder sample in 30 mL of deionized water, and 5% nitric acid and diluted sodium hydroxide solutions were subsequently added to adjust the pH of the solutions. Then, 10 mL of the suspensions were loaded into the sample cell, and zeta potential of the modified derivative BTU-SS at different pH values was measured likewise. The elemental composition (i.e., C, H, N, and S) of the biosorbents was determined by elemental analysis (Elementar Vario EL III), while the specific surface area and pore volume were determined by nitrogen physisorption (Micromeritics ASAP 2460). In order to evaluate the amount of functional groups available for modification, titration of amino end-groups on SS was carried out. First, 2.0 g of SS were dissolved in 100 mL of boiling deionized water and cooled down to room temperature, and then 25 mL of the SS solution (20 g·L^{-1}) were measured and titrated with 0.01 M HCl in a 100 mL conical flask with methyl red (0.4g·L^{-1}) as an indicator and deionized water as a blank. The total organic carbon (TOC) content was analyzed on a TOC analyzer (Elementar Vario TOC cube analyzer). Surface analyses of the fresh and spent biosorbents

were carried out by X-ray photoelectron spectroscopy (XPS, Thermo Scientific K-Alpha) using a monochromatic Al X-ray source (1486.6 eV) at 350 W (14 kV; 25 mA) and a vacuum of 1×10^{-8} Torr operating in the constant analyzer energy (CAE) mode. The powder sample was slightly dusted on adhesive tape and carefully mounted for analysis. A low-energy electron flood gun was used to compensate the XPS-induced surface charging effects. The data were plotted with respect to the binding energy, which was referenced to the C1s line (284.6 eV) corresponding to adventitious carbon. The curve deconvolution of the obtained spectra was performed with the XPS peak fitting program.

2.3 Adsorption and Separation Experiments

Batch single and multi-metallic adsorption experiments were carried out at room temperature (298 ± 2 K) in a shaker bath using 0.14 g of either SS or BTU-SS with 40 mL of aqueous solutions. Both the initial and final metallic ion concentrations in solution before and after adsorption were analyzed on an atomic absorption spectrophotometer (Thermo Scientific S SERIES AA) previously calibrated with standard solutions before each set of analyses. The TOC was measured to determine the amount of soluble organic carbons in solution. The adsorption capacity, q_e (mg·g^{-1}), was calculated from Equation 1:

$$q_e = \frac{(C_o - C_e) \cdot V}{m} \qquad (1)$$

where C_o (mg·L^{-1}) and C_e (mg·L^{-1}) are the initial and final metal concentrations, respectively, V (L) is the solution volume, and m (g) is the mass of adsorbent.

The selective adsorption of Ag was demonstrated using a multi-component leachate. The actual leachate was obtained from printed circuit boards. The printed circuit boards were first mechanically smashed and calcined at 1073 K for 4 h to remove the plastic components. The powdered residue was subsequently leached with nitric acid, and the leachate obtained was neutralized to approximate pH = 3.0 for the convenience of the subsequent tests. The measured concentrations of some major elements in the leachate were: Cu(II) = 602.3; Ni(II) = 534.8; Pb(II) = 398.7; Zn(II) = 53.8; and Ag(I) = 113.6 mg·L^{-1}.

The percent removal η (%) of the metallic ions (Eq. 2) was determined from the atomic absorption spectrophotometer analyses as follows:

$$\eta(\%) = \frac{(C_o - C_e)}{C_o} \times 100 \qquad (2)$$

2.4   Continuous Column Tests

Continuous column tests were carried out using a small glass column with a height of 26.0 cm and an internal diameter of 0.8 cm. These tests were carried out to evaluate the suitability of BTU-SS for the selective adsorption of Ag(I) from an e-waste leachate in the presence of coexisting metallic ions at higher concentrations. In a typical experiment, 0.4 g of BTU-SS were dipped into deionized water for a few hours before being packed in the glass column. The packed bed was first fitted with deionized water for 2 h and followed by diluted HNO_3 (pH = 3.0) for 10 h. The leachate at pH = 3.0 containing certain concentrations of Cu(II), Ni(II), Pb(II), Zn(II), and Ag(I) was penetrated upward through the packed bed at a constant flow rate of 5.0 cm^3 h^{-1} using a peristaltic pump (BT100S, Baoding Leifu, China). The effluent was periodically sampled on a fraction collector (SBS-100, Shanghai Huxi, China) and analyzed at hourly intervals to determine the residues of various metallic ions in the effluent with the atomic absorption spectrophotometer. The volume of BTU-SS used herein was 0.5 cm^3, and the liquid hourly space velocity (LHSV) was 10.0 h^{-1}.

Once the loaded Ag(I) was saturated, the BTU-SS packed bed was first washed with deionized water, and the adsorbed metallic ions were eluted with an acidic solution of thiourea (1.0 M thiourea in 1.0 M HNO_3) with an elution rate of 10 cm^3 h^{-1} using the peristaltic pump indicated above. The eluted solution was also periodically sampled and analyzed at hourly intervals, and the metallic ion concentrations in the eluted solution were likewise analyzed. After the elution of the adsorbed metals, the BTU-SS material was regenerated and used for the next cycle.

In the case of the samples, the experiments were performed in triplicate. For each set of data analyzed, the mean values and standard errors were determined and used to show the error bars in the figures.

3   RESULTS AND DISCUSSION

3.1   Biosorbent Characterization

3.1.1   FTIR Spectra of SS and BTU-SS

Figure 1 shows the infrared spectra of SS and BTU-SS. The peaks at ca. 2937 and 3440 cm^{-1} were attributed to the N-H stretching vibration of amides A and B, respectively, while the peak at ca. 1650 cm^{-1} was ascribed to amide I and believed to originate from the stretching vibrations of C=O. The peak at 1533 cm^{-1} was produced by the in-plane N-H bending of amide II. The above-mentioned peak positions were in agreement with those reported by Gulrajani et al. [25]. The

peaks at 1400, 1242, 1071, and 1078 cm^{-1} were assigned to the C-N stretching vibration, the N-H bending, and the combination of C=S and C-OH stretching vibration bands, respectively. The broad absorption band in the range of 3446–3288 cm^{-1} arose from the O-H and N-H stretching vibrations.

After the BTU grafting process, significant changes were observed in the FTIR spectra. The peak at 1551 cm^{-1} was attributed to the stretching vibration of the N-C-N bond. The weak peak at 669 cm^{-1} was ascribed to the stretching vibration of N–C=S, while the peak at 1462 cm^{-1} was attributed to the C=S band of thioamide [26], thereby revealing the presence of C=S groups in the structure of BTU-SS.

The spectroscopic analyses showed that both biosorbents were rich in carboxyl, carbonyl, hydroxyl, sulphonyl, and amino groups. These structural characteristics of SS and its BTU-SS derivative make them suitable for adsorbing precious metals via complexation.

3.1.2   Zeta Potential Measurements of SS and BTU-SS

Figure 2 displays the zeta potential for SS and its modified BTU-SS derivative. In line with previous results [12,27], SS showed an isoelectric point of ca. 3.7. Sericin has a positively charged surface at low pH values since its acidic condition favors the protonation of the surface amino groups. At pH values higher than 3.7, sericin has a negatively charged surface as a result of the deprotonation of the carboxyl groups. BTU-SS showed a somewhat lower isoelectric point (ca. 3.0) as compared to SS, and this result indicated that the modified sample possessed a wider pH range for the
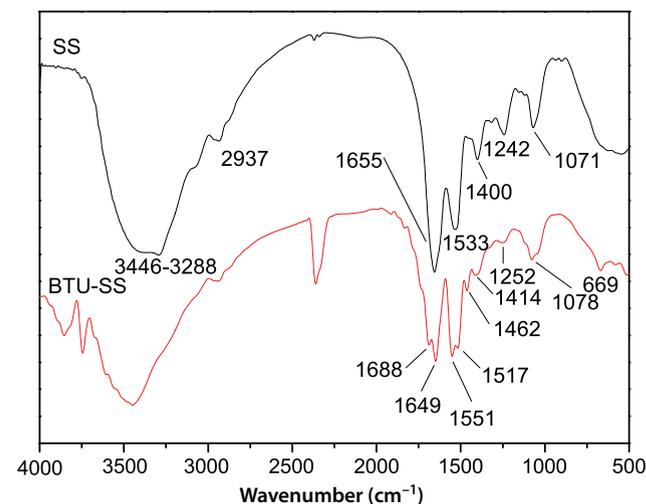

Figure 1 FTIR spectra of SS and BTU-SS.

adsorption of cations (i.e., a negatively charged surface in solution for pH values higher than 3.0).

3.1.3 Elemental Analysis

The IR spectra provided qualitative information on the immobilization of functional groups over the surface of SS. This information (i.e., the degree of functional groups grafted on the surface of BTU-SS) was quantitatively corroborated via elemental analysis. The elemental compositions of SS and BTU-SS are presented in Table 1. Titration results corresponding to the amino end-groups on SS are also listed in Table 1.

As shown in Table 1, BTU-SS showed significantly higher S and N contents than SS, thereby confirming the successful grafting of S- and N-containing functional groups on the surface of SS. Also, among the total N-containing groups, ca. 3.1% corresponded to amino end-groups. As soft ligand sites, the immobilized S and N atoms are anticipated to play a key role in binding soft Ag(I) species.

3.1.4 Brunauer–Emmett–Teller (BET) Surface Area and TOC Analysis

In line with the results reported by Chen *et al.* [12], nitrogen physisorption results revealed BTU-SS to be nonporous (BET surface area of merely 0.24 m²·g⁻¹),
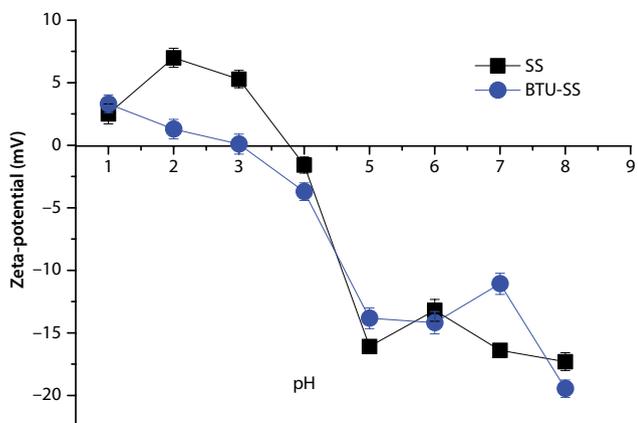

Figure 2 Zeta potential of SS and BTU-SS at different pH.

thereby implying that the grafted functional groups were mainly responsible for the adsorption ability of BTU-SS.

The TOC measurements can provide an indication of the content in soluble organic matter in water. SS and BTU-SS showed TOC values of 9.329 and 0.549 mg·L⁻¹, respectively. Thus, the TOC value of BTU-SS decreased by ca. 94% after the chemical modification of SS, which was also effective in decreasing the solubility of the modified sample.

3.2 Adsorption Behavior of SS and BTU-SS towards Ag(I) in a Single-Component Solution

In order to obtain the optimal conditions for the biosorption of Ag ions, the effects of different variables on the biosorption process were evaluated. The main variables studied were contact time, biosorbent dose, solution pH, and temperature. The experiments were performed at ambient temperature (300 K) unless otherwise specified.

3.2.1 Effect of the Contact Time

The effect of the contact time was analyzed at an initial Ag(I) concentration of 108.0 mg·L⁻¹ with a biosorbent dose of 3.5 g·L⁻¹ at pH = 5.0, and the results are shown in Figure 3. The amount of adsorbed Ag(I) first increased dramatically (0–2 h) and then slowly (2–15 h) before leveling off around the equilibrium value. The rapid Ag(I) adsorption during the initial stage was probably caused by the availability of abundant adsorption vacant active sites on the surface. After that period, adsorption on the remaining vacant sites was gradually hindered as a result of the repulsive forces between the Ag ions on the biosorbent and the bulk phases [28]. The adsorption percentages at equilibrium for SS and BTU-SS towards Ag(I) were 58.5 and 98.3%, respectively, corresponding to adsorption capacities of 18.0 and 30.3 mg·g⁻¹. Thus, the adsorption properties of the chemically modified BTU-SS biosorbent were greatly improved. BTU-SS exhibited a fairly good adsorption capacity towards
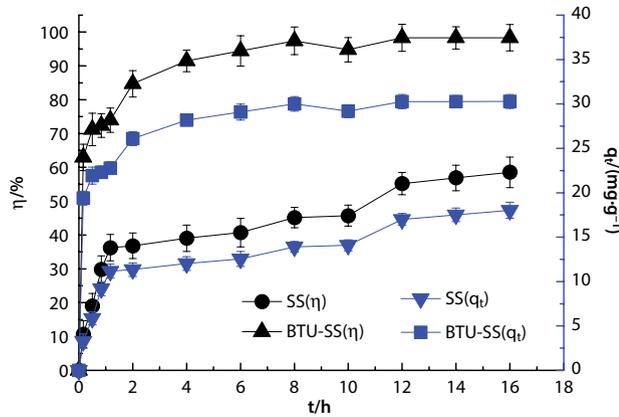
Table 1 Elemental composition of SS and BTU-SS.

Biosorbent	Elements/(wt%)				Total N-containing groups* (mmol·g⁻¹)	Amino end-groups** (mmol·g⁻¹)
	C	H	N	S		
SS	39.86	6.033	13.45	0.254	9.61	0.30
BTU-SS	39.51	5.999	14.46	1.948	–	–

*This data is calculated based on nitrogen content determined from elemental analysis.
**This data is measured by titration.

Figure 3 Effect of contact time on adsorption of Ag(I); (pH = 5.0, biosorbent dose = 3.5 g·L^{-1}, C_0(Ag(I)) = 108.0 mg·L^{-1}).
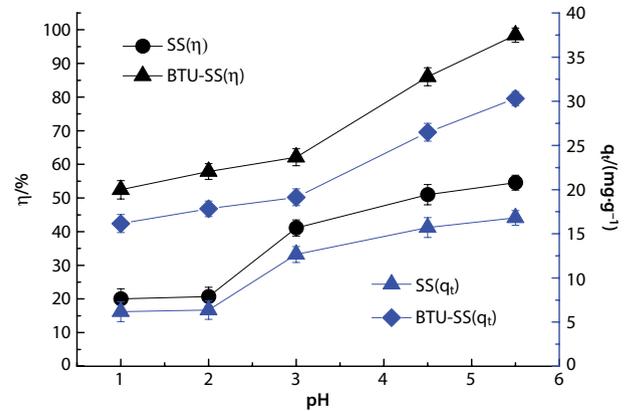
Figure 5 Effect of pH on adsorption of Ag(I); (t = 15 h, biosorbent dose = 3.5g·L^{-1}, C_0(Ag(I)) = 108.0 mg·L^{-1}).
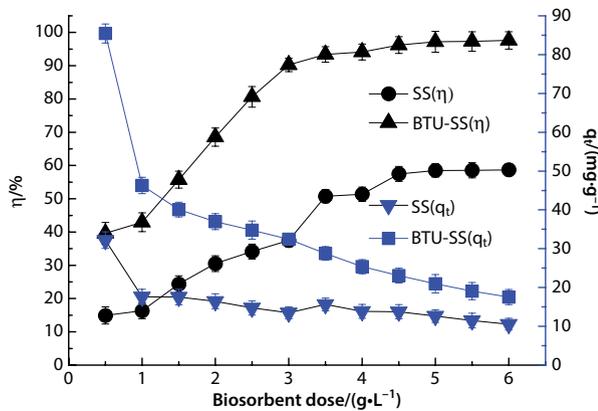

Figure 4 Effect of biosorbent dose on adsorption of Ag(I); (pH = 5.0, t = 15 h, C_0(Ag(I)) = 108.0 mg·L^{-1}).

Ag(I) as compared with the limited literature reports available (i.e., maximum adsorption capacities towards Ag(I)) on fungi *Cladosporium cladosporioides* Strain 1 [29] (43.1 mg·g^{-1}), *Cladosporium cladosporioides* Strain 2 [29] (12.9 mg·g^{-1}), and yeast *Saccharomyces cerevisiae* [30] (41.7 mg·g^{-1}).

3.2.2   Effect of the Biosorbent Dose

The dose of biosorbent has a great effect on the biosorption process. The effect of the biosorbent dose on the adsorption percentage and the capacity towards Ag(I) is shown in Figure 4.

The adsorption percentage increased with the amount of biosorbent added. Thus, higher doses are equivalent to an increase in the surface area, which in turn increases the number of binding sites. However, on the other hand, the adsorption capacity (i.e., the amount of adsorbed solute per unit mass of biosorbent) decreased with the biosorbent dose. This result

can be explained by the lack of solute available to completely occupy the available exchangeable sites on the biosorbent at high biosorbent doses, thereby leading to poor solute biosorption [31]. In addition, as reported by Gadd *et al.* [32], competitive adsorption and mutual interference between binding sites at high biosorbent doses can also result in lower adsorption capacities for the biosorbents, in line with the results reported by Esposito *et al.* [33] and Song *et al.* [34] for other adsorption systems. Thus, to efficiently and economically utilize the biosorbents, both the adsorption percentage and the adsorption capacity must be taken into account. The SS and BTU-SS doses used herein for the batch experiments (3.5 g·L^{-1}) achieved both optimum adsorption percentage and capacity values. Also, as clearly shown in Figure 4, BTU-SS showed superior adsorption capacity to that of SS.

3.2.3   Effect of the Solution pH

The solution pH is one of the most important parameters influencing the metal species in solution [35] and could affect both the dissociation state of the binding site and the solution chemistry of the metal adsorbed in terms of hydrolysis, coordination, and redox potentials [36]. Figure 5 shows the adsorption of Ag(I) on SS and BTU-SS at varying pH values. The results showed that the adsorption capacity of both biosorbents towards Ag(I) increased with the solution pH, in line with the zeta potential results (Figure 2). Thus, the zeta potential measurements of SS and BTU-SS revealed that both biosorbents contained positively charged surface groups at pH values lower than 3.0 as a result of the protonation of surface functional moieties. Thus, the adsorption of positively charged Ag ions was inhibited at low pH values. In contrast, at higher pH values, the presence of negatively charged

surface groups on the biosorbents was beneficial to adsorb positively charged Ag ions via charge interactions. However, with the aim of preventing the precipitation of Ag(I), pH values above 5.0 should be avoided.

3.2.4 Effect of the Temperature

Figure 6 shows the adsorption of Ag(I) on the biosorbents at different temperatures (298–328 K). The adsorption percentages decreased with increasing temperature for both SS and BTU-SS, thereby indicating that the adsorption process was exothermic. However, this decrease was not significant (from 58.5 to 50.7% for SS and from 98.3 to 91.3% for BTU-SS upon increasing temperature from 298 to 328 K, respectively), thereby allowing the biosorption to be carried out at ambient temperature.
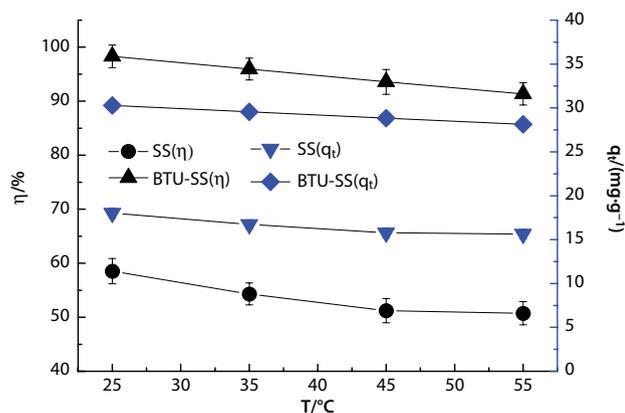

Figure 6 Effect of temperature on adsorption of Ag(I); (t = 15 h, pH = 5.0, biosorbent dose = 3.5 g·L^{-1}, C_0(Ag(I)) = 108.0 mg·L^{-1}).

3.3 Ag Separation from a Multi-component E-Waste Leachate

As described in Section 2.3, the biosorbents were further tested for the separation of Ag(I) from a five-component (Ag(I)-Cu(II)-Zn(II)-Ni(II)-Pb(II)) e-waste leachate. As can be seen in Table 2, although the adsorption percentages of the coexisting metallic base cations on both SS and BTU-SS were relatively low in the five-component solution, SS exhibited poor selectivity towards Ag(I), in line with previous results [12]. In contrast, BTU-SS exhibited superior selectivity towards Ag(I) to that of SS in the presence of base metallic ions. Thus, the adsorption percentage of SS towards Ag(I) at pH = 5.0 only reached 32.0% (10.4 mg·g^{-1}), which is lower than that obtained in the single Ag(I) system at a comparable concentration. In contrast, BTU-SS showed an adsorption percentage towards Ag(I) of 93.9% (30.5 mg·g^{-1}) at similar conditions, and this value was nearly that obtained in the single Ag(I) system at comparable concentrations. Thus, Ag(I) could be selectively separated from the coexisting base metal ions using BTU-SS.

The larger affinity of BTU-SS towards Ag(I) versus other cations allowed a selective Ag(I) biosorption process in multi-component leachates and its separation from e-waste leachates. As mentioned above, Ag(I) is a soft acid according to the Pearson's HSAB principle, and the functional moieties of BTU-SS are rich in soft base species, thereby explaining the superior selectivity towards Ag(I) of BTU-SS.

3.4 Adsorption Kinetics

To investigate the biosorption mechanism of Ag(I) onto SS and BTU-SS, adsorption kinetic studies

Table 2 Adsorption percentages of SS and BTU-SS in Ag(I)-Cu(II)-Zn(II)-Ni(II)-Pb(II) system at pH 3.0 and pH 5.0.

Metallic ions	pH	C_0/(mg·L^{-1})	SS		BTU-SS	
			C_e/(mg·L^{-1})	η/(%)	C_e/(mg·L^{-1})	η/(%)
Ag(I)	3.0	113.6	73.2 ± 2.7	35.6 ± 2.4	9.3 ± 2.8	91.8 ± 2.5
	5.0		77.3 ± 2.5	32.0 ± 2.2	6.9 ± 2.4	93.9 ± 2.1
Cu(II)	3.0	602.3	575.8 ± 6.6	4.4 ± 1.1	602.8 ± 7.2	0.0 ± 1.2
	5.0		594.6 ± 10.8	1.3 ± 1.8	602.6 ± 7.8	0.0 ± 1.3
Zn(II)	3.0	53.8	49.1 ± 1.3	8.7 ± 2.4	51.5 ± 1.2	4.3 ± 2.2
	5.0		49.6 ± 1.5	7.8 ± 2.8	51.2 ± 1.3	4.8 ± 2.4
Ni(II)	3.0	534.8	529.8 ± 5.3	0.9 ± 1.0	535.8 ± 4.3	0.0 ± 0.8
	5.0		520.3 ± 5.9	2.7 ± 1.1	518.2 ± 4.8	3.1 ± 0.9
Pb(II)	3.0	398.7	372.5 ± 5.2	6.6 ± 1.3	395.3 ± 6.4	0.9 ± 1.6
	5.0		377.6 ± 6.8	5.3 ± 1.7	393.6 ± 7.2	1.3 ± 1.8

were conducted to understand the kinetic behavior of biosorbents towards Ag ions at different temperatures. As shown in Figure 7, within the first 2 h, both SS and BTU-SS showed very high Ag(I) adsorption rates. These rates increased less pronouncedly thereafter (2–15 h) before leveling off at ca. 15 h. Comparably, BTU-SS clearly showed superior adsorption performance to that of SS at the same temperature.

The adsorption kinetics of the Ag(I) uptake process over SS and BTU-SS were studied by applying widely used kinetic models such as the Lagergren pseudo-first-order [37] and the pseudo-second-order [38].

The linear expression of the Lagergren pseudo-first-order model is given by Equation 3:

$$\lg\left(q_e - q_t\right) = \lg q_e - \frac{k_1 t}{2.303} \tag{3}$$

where k_1 (h^{-1}) is the rate constant for the pseudo-first-order adsorption, and q_e and q_t (mg g^{-1}) are the adsorption capacities at equilibrium and at time t (h), respectively. k_1, q_e, and the correlation coefficient R^2 could be calculated by using the slope and intercept from the $\lg(q_e - q_t)$ versus t plots (figure not shown because of poor linearity).

The pseudo-second-order kinetic equation is probably the most frequently used kinetic model describing the adsorption kinetics at solid/solution interfaces. This model assumes the presence of chemisorption phenomena involving valence forces (e.g., ion exchange and sharing or exchange of electrons) between the adsorbent and the metal ions adsorbed [38-41].

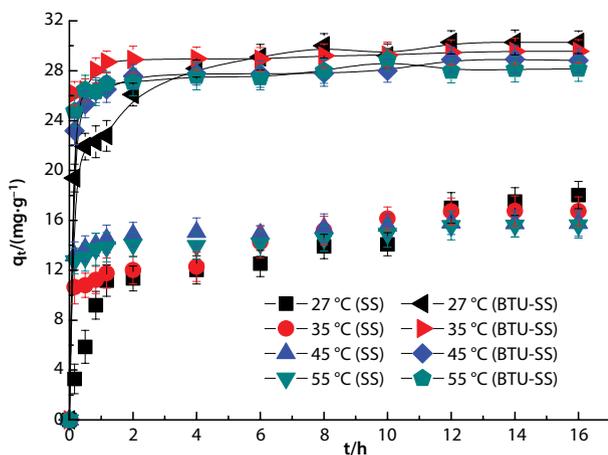The adsorption of Ag(I) on SS and BTU-SS may involve chemical adsorption processes. The linear expression of the pseudo-second-order equation is given in Equation 4:

$$\frac{t}{q_t} = \frac{1}{k_2 q_e^2} + \frac{1}{q_e} t \tag{4}$$

where q_e and q_t (mg·g^{-1}) are the adsorption capacities at the equilibrium and time t (h), and k_2 (g·mg^{-1}·h^{-1}) is the rate constant of the pseudo-second-order adsorption process. k_2, q_e, and the correlation coefficients R^2 were calculated from the linear plots of t/q_t versus t (as shown in Figure 8).

The linear fitted results and the obtained kinetic parameters are summarized in Table 3. The R^2 values suggested that the pseudo-second-order model was more suitable than the pseudo-first-order model for describing the adsorption kinetics of Ag(I) on both SS and BTU-SS, and the adsorption capacities predicted by this model were well matched with those obtained experimentally. Figure 8 shows the fitting of the pseudo-second-order kinetics for the biosorbents SS and BTU-SS. It could be concluded that the adsorption of Ag(I) on SS and BTU-SS followed a pseudo-second-order kinetic, which implies that the adsorption mainly involved chemisorption phenomena (i.e., share of electrons between the ligand atoms on the biosorbent and the adsorbed Ag(I) to form complexes).

The relationship between the pseudo-second-order rate constant k_2 and the temperature may be described by the Arrhenius equation (Eq. 5):

$$k_2 = A\exp\left(-E_a/RT\right) \tag{5}$$

where A (g·mg^{-1}·h^{-1}) is the temperature-independent factor, E_a (kJ·mol^{-1}) is the activation energy for the biosorption process, R is the gas constant

Figure 7 Adsorption kinetics of SS and BTU-SS towards Ag(I) at different temperatures; (pH = 5.0, biosorbent dose = 3.5 g·L^{-1}, C_0(Ag(I)) = 108.0 mg·L^{-1}).
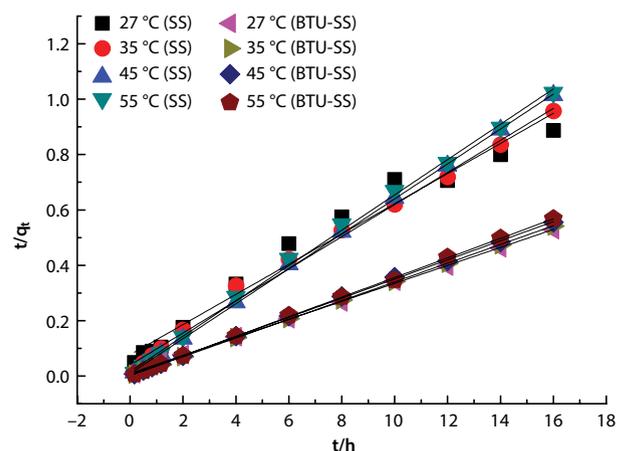

Figure 8 The fitting of pseudo-second-order for adsorption of Ag(I) onto SS and BTU-SS at different temperatures.

Table 3 Adsorption kinetic parameters of Ag(I) onto SS and BTU-SS.

| Biosorbent | $T/°C$ | Pseudo-first-order | | | Pseudo-second-order | | | Activation energy |
		$k_1/(\text{h}^{-1})$	$q_e/(\text{mg·g}^{-1})$	R^2	$k_2/(\text{g·mg}^{-1}\text{·h}^{-1})$	$q_e/(\text{mg·g}^{-1})$	R^2	$E_a/(\text{kJ·mol}^{-1})$
SS	27	0.1876	12.6	0.8443	0.0386	18.3	0.9708	53.27
	35	0.3603	10.2	0.8753	0.0844	17.3	0.9933	
	55	0.0750	3.6	0.9088	0.2484	15.8	0.9980	
BTU-SS	27	0.5346	14.0	0.9714	0.1103	30.8	0.9981	47.67
	45	0.2063	3.6	0.8419	0.2693	28.9	0.9996	
	55	0.3213	2.4	0.8648	0.5789	28.3	0.9997	
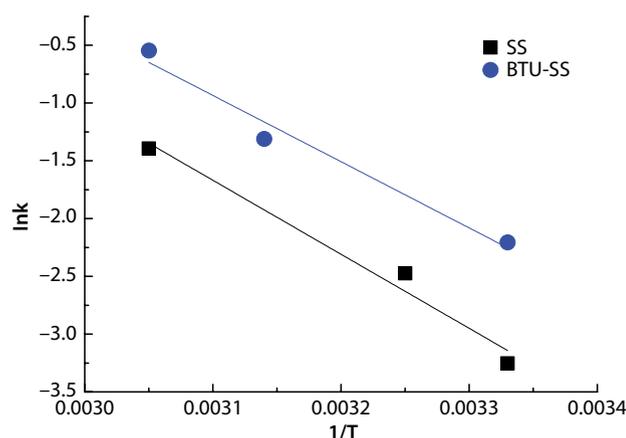
**Figure 9** Relationship between $1/T$ and $\ln k$ for adsorption of Ag(I) onto SS and BTU-SS.

(8.314 $\text{J·mol}^{-1}\text{·K}^{-1}$), and T (K) is the absolute temperature. E_a could be calculated from the slope $(-E_a/R)$ of the $\ln k$ versus $1/T$ linear plot (Figure 9).

The magnitude of E_a may provide an indication of the type of adsorption process involved (i.e., physisorption or chemisorption). Thus, an E_a value higher than 40 kJ·mol^{-1} is generally associated with a chemisorptive process [42]. The calculated E_a values (Table 3) for SS and BTU-SS were 53.27 and 47.67 kJ·mol^{-1}, respectively; thereby confirming the chemisorptive nature of the biosorption of Ag(I) over SS and BTU-SS.

3.5 Thermodynamic Parameters of the Biosorption Process

To prove the effectiveness of SS and BTU-SS for the adsorption of Ag(I), a thermodynamic study was performed by calculating the Gibbs free energy change (ΔG^Θ), the enthalpy change (ΔH^Θ), and the entropy change (ΔS^Θ) of the biosorption process. This study allowed evaluation of the thermodynamic feasibility and spontaneity of the adsorption process.

The adsorption process of Ag(I) on the biosorbents can be simplified by the following reversible process which represents a heterogeneous equilibrium:

$$\text{Ag(I) (aq) + Biosorbent(s)} \rightleftharpoons \text{Ag(I)} - \text{Biosorbent(s)}$$
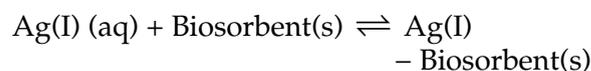
The apparent equilibrium constant (K_d) of the biosorption system is actually the partition coefficient of the solute between the solid and aqueous phases. This physical quantity, whose dimension is 1, could be defined by Equation 6 [43]:

$$K_d = \frac{(C_o - C_e) \cdot V/m}{V \cdot C_e / (\rho \cdot V \cdot 10^3)} = \frac{q_e}{C_e} \cdot 10^3 \quad (6)$$

where C_o (mg·L^{-1}) and C_e (mg·L^{-1}) are the initial and equilibrium Ag(I) concentrations, respectively, V (L) is the solution volume, m (g) is the mass of biosorbent, q_e (mg·g^{-1}) is the adsorption capacity, and ρ (g·mL^{-1}) is the density of water (1.0 g·mL^{-1}).

Thermodynamically, ΔG^Θ is related to the standard thermodynamic equilibrium constant (K_D^Θ) via Equation 7:

$$\Delta G^\Theta = -RT \ln K_D^\Theta \quad (7)$$

Theoretically, the activity should be used in replacement of the concentration term of Equation 6 to obtain K_D^Θ via the infinite dilution value of K_d, which can be obtained by calculating K_d at different initial concentrations of Ag(I) and extrapolating to zero. However, for diluted solutions, the utilization of concentration instead of activity would not lead to a significant error. Herein, C_o was as low as 108.0 mg·L^{-1}, and letting alone C_e and taking K_d as K_D^Θ would be a satisfactory approximation.

K_D^Θ could be expressed as a function of temperature by the van 't Hoff equation (Eq. 8):

$$\ln K_D^\Theta = -\frac{\Delta G^\Theta}{RT} = -\frac{\Delta H^\Theta}{RT} + \frac{\Delta S^\Theta}{R} \quad (8)$$

$\Delta H^{\ominus}$ and $\Delta S^{\ominus}$ could be obtained by calculating the slope and intercept from the $\ln K_D^{\ominus}$ versus $1/T$ van 't Hoff plot (Figure 10).

Table 4 presents the thermodynamic parameters. The negative $\Delta G^{\ominus}$ values at all the experimental temperatures indicated that the biosorption of Ag(I) was spontaneous. The negative values of $\Delta H^{\ominus}$ suggested the exothermic nature of the process.

$\Delta S^{\ominus}$ of the adsorption process depends upon two counteracting effects. On one hand, the diffusion of Ag(I) from the bulk solution to the biosorbent surface would increase the order of the system (i.e., lower entropy values). On the other hand, the surface of the biosorbents underwent some structural changes during the adsorption process (i.e., some water molecules adsorbed on the surface were replaced by the silver ions). In this process, the translational entropy gained by the released water molecules surpasses that lost by the adsorbed silver ions, thus increasing the randomness of the system [44]. If the former effect dominates the adsorption process, $\Delta S^{\ominus}$ would be negative, thereby suggesting an decrease in the randomness at the solid/solution interface during the biosorption process (adsorption of Ag(I) on BTU-SS is the right

Figure 10 Van 't Hoff relationship between $1/T$ and $\ln K_D^{\ominus}$ for adsorption of Ag(I) onto SS and BTU-SS.

example for such a case). However, if the latter effect making the entropy of the system increase prevails over the former effect (leading to lower entropy values), $\Delta S^{\ominus}$ would be positive and the randomness at the solid/solution interface would increase during the biosorption process (adsorption of Ag(I) on SS is the right example for such a case).

3.6 Continuous Column Adsorption and Elution Experiments

The batch adsorption experiments revealed that BTU-SS has a noticeable selectivity towards Ag ions in the presence of coexisting base metallic ions in an acidic e-waste leachate. The feasibility of BTU-SS to selectively separate and recover Ag(I) from an e-waste leachate was evaluated by performing continuous column mode experiments followed by elution.

Breakthrough curves intuitively reflect the adsorption relationship between mobile and stationary phases in a column adsorption process. These curves also serve as the basis for the operation and control of adsorption processes at industrial scale. Figure 11a displays the breakthrough curves for the various metallic ions under investigation over a BTU-SS-packed column. Rapid breakthroughs were observed for Cu(II), Ni(II), Zn(II), and Pb(III) ions, thereby indicating that these coexisting metallic ions passed through the packed bed quickly without being adsorbed on BTU-SS. Unlike these coexisting metals, a zigzag breakthrough curve was obtained for Ag(I), which was indicative of a breakthrough adsorption (C_t/C_0 = 0.1) on the BTU-SS-packed bed, with breakthrough occurring at 130 bed volumes (BV, equivalent to 13 h) and saturation being reached at 260 BV (26 h). These results indicated that BTU-SS has a strong affinity towards Ag(I) which, in turn, facilitates the separation of Ag(I) from the coexisting base metals under continuous operation. The adsorption capacity towards Ag(I), calculated from the breakthrough curves, was lower (22.5 mg·g^{-1}) than the equilibrium adsorption capacity obtained in the batch experiments. This difference can
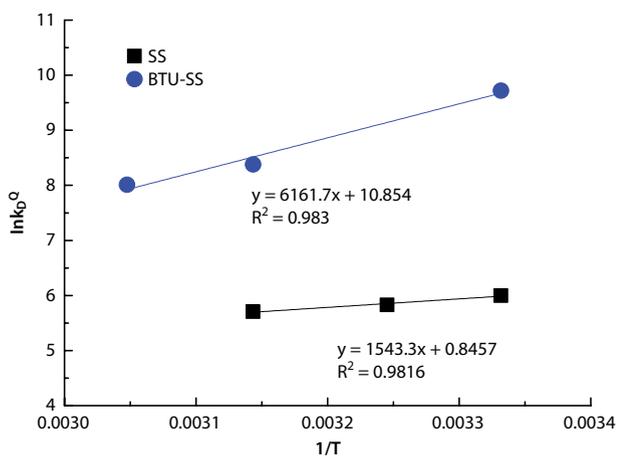
Table 4 Adsorption thermodynamic parameters of Ag(I) onto SS and BTU-SS.

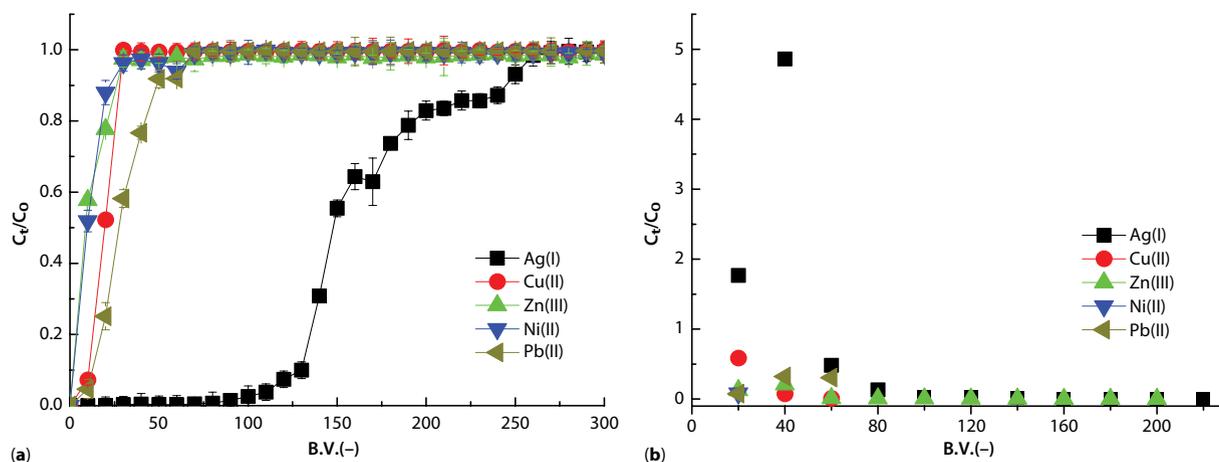| Biosorbent	T/K	$K_D^{\ominus}$	$\Delta G^{\ominus}$/(kJ·mol^{-1})	$\Delta H^{\ominus}$/(kJ·mol^{-1})	$\Delta S^{\ominus}$/(J·mol^{-1})
SS	300	403.3	−14.97	−12.83	7.03
	308	340.7	−14.94		
	318	301.0	−15.10		
BTU-SS	300	16634.6	−24.25	−51.23	−90.24
	318	4360.0	−22.17		
	328	3013.6	−21.86		

Figure 11 Breakthrough curves (**a**) and elution curves (**b**) of metallic ions on BTU-SS in Ag(I)-Cu(II)-Zn(II)-Ni(II)-Pb(II) system. (Feed concentrations of metallic ions (mg·L^{-1}): Cu(II) = 602.3; Ni(II) = 534.8; Pb(II) = 398.7; Zn(II) = 53.8; Ag(I) = 113.6 with flow rate 5.0 cm^3·h^{-1}; Eluent = 1.0 M thiourea in 1.0 M HNO$_3$ with elution rate 10.0 cm^3·h^{-1}.)

be mainly ascribed to a synergistic effect caused by: (i) the competitive adsorption of the various metallic ions; (ii) the lack of time for metallic ions to contact with the biosorbent; and (iii) the channeling flow of the feed solution [12, 15–17].

Once the amount of Ag(I) adsorbed reached the saturation point, the BTU-SS-packed bed was eluted with a 1.0 M thiourea solution in 1.0 M HNO$_3$ to recover the adsorbed Ag(I) (Figure 11b). Ag(I) was eluted within 2 h with a preconcentration factor of 4.9, and 92.2% of the adsorbed Ag(I) was eluted within 8 h, thereby suggesting that the elution process was quite efficient.

3.7 Regeneration and Reusability Tests of BTU-SS

The reusability and stability properties of BTU-SS were assessed by performing successive adsorption/elution cycles in a continuous column mode. As described in Section 2.4, the e-waste leachate passed through the BTU-SS-packed column until the amount of adsorbed Ag(I) reached the saturation point. The Ag ions adsorbed on BTU-SS were subsequently eluted with a 1.0 M thiourea solution in 1.0 M HNO$_3$ to regenerate the biosorbent. The regenerated BTU-SS material was subsequently fitted with diluted HNO$_3$ (pH = 3.0) for 2 h prior to the next adsorption cycle. This process was repeated four times to perform consecutive adsorption/elution cycles, and the results are illustrated in Figure 12. BTU-SS showed superior durability and good adsorption characteristics toward Ag ions even after four repeated adsorption/elution cycles. Consequently, BTU-SS can be potentially used to recover Ag from various silver-containing industrial effluents.
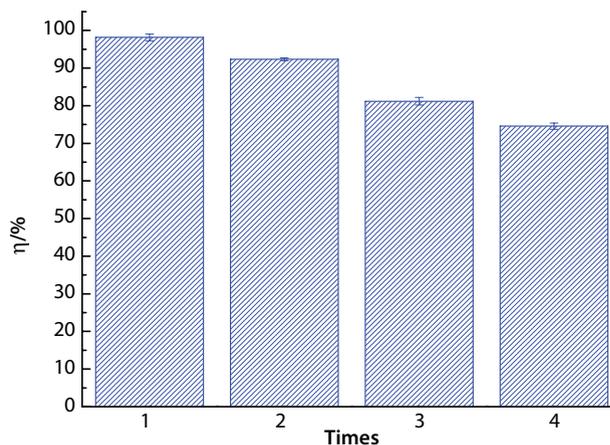

Figure 12 Plot of reusability of regenerated BTU-SS.

3.8 Potential Biosorption Mechanism

As shown in Figure 2, under acidic conditions (i.e., pH values lower than the isoelectric point) the nitrogen atoms of BTU-SS are easily converted into positively charged centers (quaternary ammonium groups). This protonation hindered the adsorption of cationic Ag(I) species, negatively affecting the biosorption of Ag(I). At pH values above the isoelectric point, the S atoms of the biosorbents can be converted into negatively charged centers (Scheme 2), thereby favoring the attraction of positively charged Ag ions by electrostatic interaction.

Most of the functional groups containing N and S atoms could act as mono-, bis-, and poly-dentate ligands to form complexes with Ag(I). Since Ag(I) is a soft Lewis acid according to the Pearson's HSAB
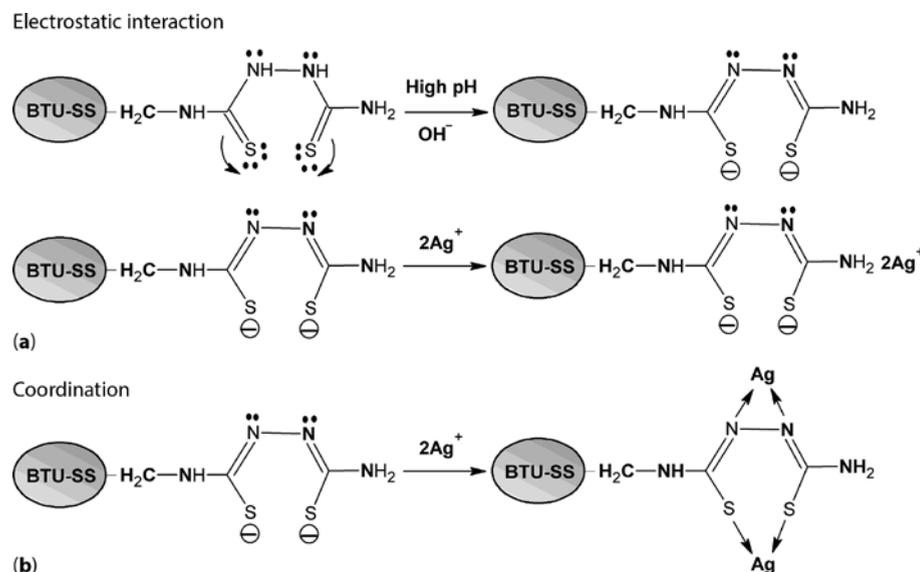
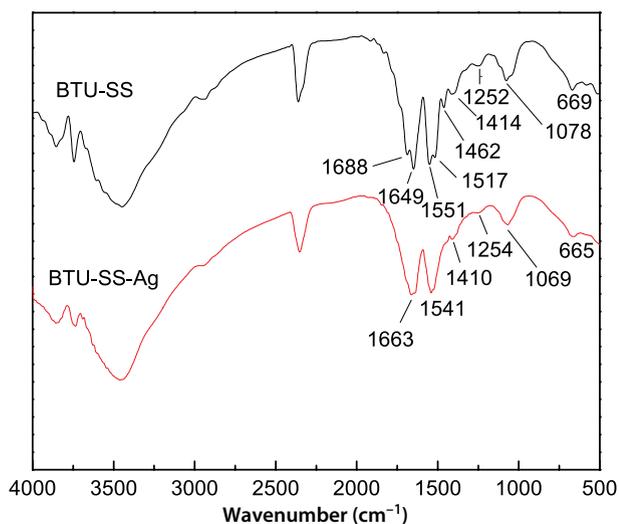**Scheme 2** Presumable mechanism of adsorption of Ag(I) on BTU-SS.

Figure 13 FTIR spectra of fresh and Ag(I)-loaded BTU-SS.

principle, the coordination between Ag(I) and these groups containing soft donor atoms is thus reasonable. Hence, as shown in Scheme 2, a potential mechanism for the biosorption of Ag(I) biosorption on BTU-SS can be proposed involving the combination of electrostatic and coordination interactions through functional groups containing N and S atoms.

The proposed adsorption mechanism was supported by the FTIR spectra (Figure 13) of fresh and Ag(I)-loaded BTU-SS samples.

As can be seen in Figure 13, significant changes were observed for the Ag(I)-loaded BTU-SS sample in the FTIR bands corresponding to C=S stretching and N-H bending vibrations. The thiocarbonyl group was

deducted to be involved in the coordination of Ag(I), as revealed by the wavenumber shift (ascribed to the binding with Ag ions) of the C=S stretching vibration. The moderate band centered at 1078 cm^{-1} (arising from the combination bands of C=S and C-OH stretching vibrations) shifted to lower wavenumbers (1069 cm^{-1}) after the adsorption process, and this was ascribed to the coordination of the thiocarbonyl group with the adsorbed Ag(I) [45]. Similarly, the in-plane N-H bending band ascribed to amide II (from 1551 to 1541 cm^{-1}) and the C=S band corresponding to thioamide (from 1462 to 1410 cm^{-1}) shifted to lower wavenumbers after Ag(I) adsorption, thereby suggesting the coordination of N-H and C=S groups with Ag(I).

The XPS analyses of fresh and Ag(I)-loaded BTU-SS samples also supported the proposed adsorption mechanism. The XPS data for the C1s, N1s, S2p, and Ag3d transitions of the BTU-SS and Ag(I)-loaded BTU-SS samples are shown in Figure 14. As shown in Figure 14a, the broad C1s peak of BTU-SS was deconvoluted into alkyl (284.8 eV), carbonyl (286.28 eV), and carboxyl (287.28 eV) species [46] typically observed in proteins. The slight increase of the C1s binding energies corresponding to carbonyl and carboxyl species after Ag(I) adsorption on BTU-SS was indicative of potential interactions between Ag(I) and these functional groups. The adsorption of metallic ions influences the local chemical environment while modifying the entire hydrophobic and hydrophilic nature of the protein [12]. This modification affects the protein folding behavior and, in turn, the accessibility of the active sites for biosorption.
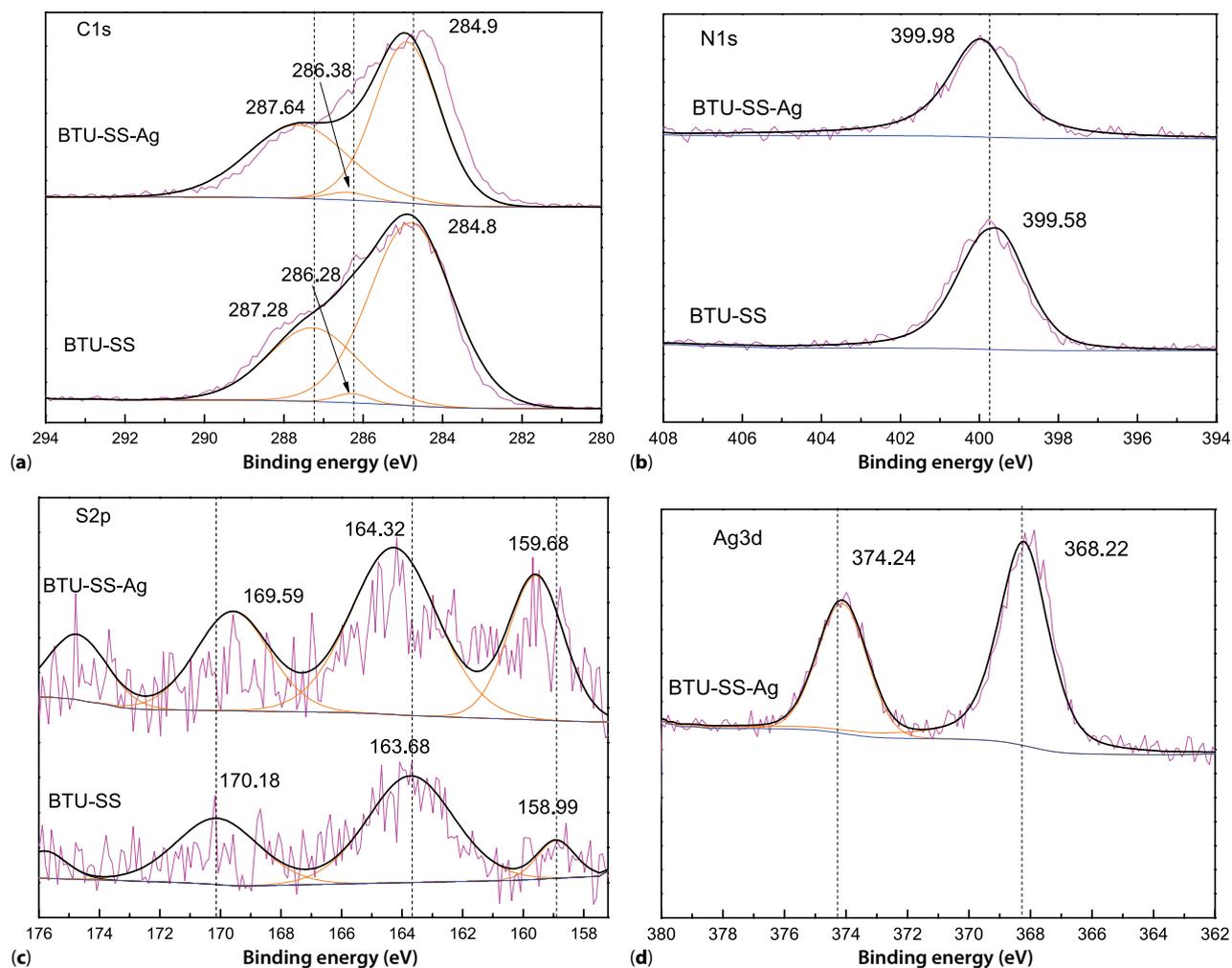
Figure 14 X-ray photoelectron spectra of fresh and Ag(I)-loaded BTU-SS: (**a**) C1s, (**b**) N1s, (**c**) S2p and (**d**) Ag3d. The observed signals with noise are shown with non-smooth curves and the fitted lines with smooth curves in all spectra.

A slight increase of the N1s binding energy (Figure 14b) was also observed after Ag(I) adsorption. The S2p band was deconvoluted (Figure 14c) and the main band at 163.68 eV was ascribed to C–S species. The binding energy of this peak slightly increased after Ag(I) adsorption, thereby suggesting possible interactions between Ag(I) and the S atom of these species. The $Ag3d_{3/2}$ (374.24 eV) and $Ag3d_{5/2}$ (368.22 eV) peaks shown in Figure 14d were typical of a silver salt [46, 47], thereby confirming the adsorption of Ag(I) on BTU-SS.

Donation of electron pairs from S2p and N1s to the unoccupied orbital of Ag(I) to form a coordination compound during the biosorption process resulted in atomic orbitals of S2p and N1s having lower density of electrons. This, in turn, increased the binding energies of S2p and N1s in the Ag(I)-loaded BTU-SS sample.

4 CONCLUSIONS

An SS-based novel BTU-SS biosorbent was prepared by grafting BTU ligands on an SS matrix. Elemental analysis and FTIR results confirmed the successful grafting of amino and thiocarbonyl groups on SS, and these groups played an active role during Ag(I) adsorption. According to the adsorption tests, the adsorption capacity of BTU-SS towards Ag(I) was greatly improved as compared to the unmodified SS material. Higher pH values favored the adsorption of Ag(I) in the pH range of 1.0–6.0. Both biosorbents (SS and BTU-SS) showed low affinity towards the coexisting cations of an Ag(I)-Cu(II)-Zn(II)-Ni(II)-Pb(II) e-waste leachate. As revealed by batch mode adsorption experiments, BTU-SS showed higher selectivity towards Ag(I) than SS in the presence of coexisting base metals. The continuous column tests with packed

BTU-SS further confirmed that Ag(I) was efficiently separated and enriched from acidic leachates in the presence of coexisting base metals. A potential mechanism explaining the selective adsorption of Ag(I) on BTU-SS was proposed involving electrostatic interactions and coordination/chelation by the thiocarbonyl and amino groups. In summary, BTU-SS displayed good adsorption capacity and excellent selectivity towards Ag, and it could be potentially used as an efficient, low-cost, and eco-friendly material for the selective recovery of Ag from various silver-containing industrial effluents. Moreover, it is reported [1,48] that the surface area and porosity of SS could be optimized by freeze-drying treatments and via formation of composites with polymers. These approaches would improve the accessibility and adsorption capacity of SS for metal adsorption. Future studies will be focused on this research line.

ACKNOWLEDGMENTS

REFERENCES

1. W. Tao, M. Li, and R. Xie, Preparation and structure of porous silk sericin materials. *Macromol. Mater. Eng.* **290**,188–194 (2005).
2. P. Aramwit, T. Siritientong, and T. Srichana, Potential applications of silk sericin, a natural protein from textile industry by-products. *Waste Manage Res.* **30**, 217–224 (2012).
3. G. Capar, S.S. Aygun, and M.R. Gecit, Treatment of silk production wastewaters by membrane processes for sericin recovery. *J. Membr. Sci.* **325**, 920–931 (2008).
4. A. Nishida, M. Yamada, T. Kanazawa, Y. Takashima, K. Ouchi, and H. Okada, Sustained-release of protein from biodegradable sericin film, gel and sponge. *Int. J. Pharm.* **407**, 44–52 (2011).
5. H. Yun, H. Oh, M.K. Kim, H.W. Kwak, J.Y. Lee, I.C. Um, S.K. Vootla, and K.H. Lee, Extraction conditions of *Antheraea mylitta* sericin with high yields and minimum molecular weight degradation. *Int. J. Biol. Macromol.* **52**, 59–65 (2013).
6. J.H. Wu, Z. Wang, and S.Y. Xu, Enzymatic production of bioactive peptides from sericin recovered from silk industry wastewater. *Process Biochem.* **43**, 480–487 (2008).
7. P. Aramwit and N. Bang, The characteristics of bacterial nanocellulose gel releasing silk sericin for facial treatment. *BMC Biotechnol.* **14**, 104 (2014).
8. S. Hofmann, C.T. Wong Po Foo, F. Rossetti, M. Textor, G. Vunjak-Novakovic, D.L. Kaplan, H.P. Merkle, and L. Meinel, Silk fibroin as an organic polymer for controlled drug delivery. *J. Control. Release* **111**, 219–227 (2006).
9. K.D. Hermanson, D. Huemmerich, T. Scheibel, and A.R. Bausch, Engineered microcapsules fabricated from reconstituted spider silk. *Adv. Mater.* **19**, 1810–1815 (2007).
10. X. Wang, E. Wenk, A. Matsumoto, L. Meinel, C. Li, and D.L. Kaplan, Silk microspheres for encapsulation and controlled release. *J. Control. Release* **117**, 360–370 (2007).
11. P. Aramwit, S. Ekasit, and R. Yamdech, The development of non-toxic ionic-crosslinked chitosan-based microspheres as carriers for the controlled release of silk sericin. *Biomed. Microdevices* **17**, 1 (2015).
12. X. Chen, K.F. Lam, S.F. Mak, and K.L. Yeung, Precious metal recovery by selective adsorption using biosorbents. *J. Hazard. Mater.* **186**, 902–910 (2011).
13. H.W. Kwak, Y. Kim, N.K. Yun, and K.H. Lee, Silk sericin microparticles as a biosorbent for hexavalent chromium ion. *Macromol. Res.* **22**, 788–795 (2014).
14. N. Das, Recovery of precious metals through biosorption—A review. *Hydrometallurgy* **103**, 180–189 (2010).
15. N.J. Creamer, V.S. Baxter-Plant, J. Henderson, M. Potter, and L.E. Macaskie, Palladium and gold removal and recovery from precious metal solutions and electronic scrap leachates by *Desulfovibrio desulfuricans*. *Biotechnol. Lett.* **28**, 1475–1484 (2006).
16. L.E. Macaskie, N.J. Creamer, A.M.M. Essa, and N.L. Brown, A new approach for the recovery of precious metals from solution and from leachates derived from electronic scrap. *Biotechnol. Bioeng.* **96**, 631–639 (2007).
17. M. Gurung, B.B. Adhikari, H. Kawakita, K. Ohto, K. Inoue, and S. Alam, Selective recovery of precious metals from acidic leach liquor of circuit boards of spent mobile phones using chemically modified persimmon tannin gel. *Ind. Eng. Chem. Res.* **51**, 11901–11913 (2012).
18. E. Romera, F. González, A. Ballester, M.L. Blázquez, and J.A. Muñoz, Biosorption with algae: A statistical review. *Crit. Rev. Biotechnol.* **26**, 223–235 (2006).
19. J. Cui and L. Zhang, Metallurgical recovery of metals from electronic waste: A review. *J. Hazard. Mater.* **158**, 228–256 (2008).
20. J. Cui and E. Forssberg, Mechanical recycling of waste electric and electronic equipment: A review. *J. Hazard. Mater.* **99**, 243–263 (2003).
21. E. Guibal, T. Vincent, and R.N. Mendoza, Synthesis and characterization of a thiourea derivative of chitosan for platinum recovery. *J. Appl. Polym. Sci.* **75**, 119–134 (2000).
22. L. Zhou, J. Liu, and Z. Liu, Adsorption of platinum(IV) and palladium(II) from aqueous solution by thiourea-modified chitosan microspheres. *J. Hazard. Mater.* **172**, 439–446 (2009).
23. A. Butewicz, K.C. Gavilan, A.V. Pestov, Y. Yatluk, A.W. Trochimczuk, and E. Guibal, Palladium and platinum sorption on a thiocarbamoyl-derivative of chitosan. *J. Appl. Polym. Sci.* **116**, 3318–3330 (2010).
24. L.J. Zhu, J. Yao, and Y. Li, Structure transformation of sericin protein dissolved from cocoon layer in hot water. *J. Zhejiang Agri. Univ.* **24**, 268–272 (1998).
25. M.L. Gulrajani, K.P. Brahma, P.S. Kumar, and R. Purwar, Application of silk sericin to polyester fabric. *J. Appl. Polym. Sci.* **109**, 314–321 (2008).

26. C.N.R. Rao, R. Venkataraghavan, and T.R. Kasturi, Contribution to the infrared spectra of organosulphur compounds. *Can. J. Chem.* **42**, 36–42 (1964).

27. R. Voegeli, Sericin silk protein: Unique structure and properties. *Cosmet. Toiletries* **108**, 101–108 (1993).

28. B.H. Hameed, I.A.W. Tan, and A.L. Ahmad, Adsorption isotherm, kinetic modeling and mechanism of 2,4,6-trichlorophenol on coconut husk-based activated carbon. *Chem. Eng. J.* **144**, 235–244 (2008).

29. A.V. Pethkar, S.K. Kulkarni, and K.M. Paknikar, Comparative studies on metal biosorption by two strains of *Cladosporium cladosporoides*. *Bioresour. Technol.* **80**, 211–215 (2001).

30. P. Simmons and I. Singleton, A method to increase silver biosorption by an industrial strain of *Saccharomyces cerevisiae*. *Appl. Microbiol. Biotechnol.* **45**, 278–285 (1996).

31. J. Tangaromsuk, P. Pokethitiyook, M. Kruatrachue, and E.S. Upatham, Cadmium biosorption by *Sphingomonas paucimobilis* biomass. *Bioresour. Technol.* **85**, 103–105 (2002).

32. G.M. Gadd, C. White, and L. De Rome, Heavy metal and radionuceotide uptake by fungi and yeasts, in *Biohydrometallurgy*, R. Norris and D.P. Kelly (Eds.), pp. 421–436, Antony Rowe Ltd., Chippenham, UK (1988).

33. A. Esposito, F. Pagnanelli, A. Lodi, C. Solisio, and F. Vegliò, Biosorption of heavy metals by *Sphaerotilus natans*: An equilibrium study at different pH and biomass concentrations. *Hydrometallurgy* **60**, 129–141 (2001).

34. H. Song, X. Li, J. Sun, X. Yin, Y. Wang, and Z. Wu, Biosorption equilibrium and kinetics of Au(III) and Cu(II) on magnetotactic bacteria. *Chin. J. Chem. Eng.* **15**, 847–854 (2007).

35. A. Esposito, F. Pagnanelli, and F. Vegliò, pH-related equilibria models for biosorption in single metal systems. *Chem. Eng. Sci.* **57**, 307–313 (2002).

36. N. Fiol, I. Villaescusa, M. Martinez, N. Miralles, J. Poch, and J. Serarols, Sorption of Pb (II), Ni (II), Cu (II) and Cd (II) from aqueous solution by olive stone waste. *Sep. Purif. Technol.* **50**, 132–140 (2006).

37. S.Y. Lagergren, Zur theorie der sogenannten adsorption gelöster stoffe. *K. Vet. Akad. Handl.* **24**, 1–39 (1898).

38. Y.S. Ho and G. McKay, Pseudo-second order model for sorption processes. *Process Biochem.* **34**, 451–465 (1999).

39. Y.-S. Ho, Review of second-order models for adsorption systems. *J. Hazard. Mater.* **136**, 681–689 (2006).

40. J. Febrianto, A.N. Kosasih, J. Sunarso, Y.-H. Ju, N. Indraswati, and S. Ismadji, Equilibrium and kinetic studies in adsorption of heavy metals using biosorbent: A summary of recent studies. *J. Hazard. Mater.* **162**, 616–645 (2009).

41. V.K. Gupta and Suhas, Application of low-cost adsorbents for dye removal—A review. *J. Environ. Manage.* **90**, 2313–2342 (2009).

42. H. Nollet, M. Roels, P. Lutgen, P. Van der Meeren, and W. Verstraete, Removal of PCBs from wastewater using fly ash. *Chemosphere* **53**, 655–665 (2003).

43. R.O.A. Rahman, H.A. Ibrahim, M. Hanafy, and N.M.A. Monem, Assessment of synthetic zeolite Na A–X as sorbing barrier for strontium in a radioactive disposal facility. *Chem. Eng. J.* **157**, 100–112 (2010).

44. H.-T. Fan, J.-B. Wu, X.-L. Fan, D.-S. Zhang, Z.-J. Su, F. Yan, and T. Sun, Removal of cadmium(II) and lead(II) from aqueous solution using sulfur-functionalized silica prepared by hydrothermal-assisted grafting method. *Chem. Eng. J.* **198–199**, 355–363 (2012).

45. U. Agarwala and L. Agarwala, Palladium and platinum complexes of quinazoline (1H,3H)-2,4-dithione-III. *J. Inorg. Nucl. Chem.* **34**, 251–258 (1972).

46. J.F. Moulder, W.F. Stickle, P.E. Sobol, and K.D. Bomben, *Handbook of X-ray Photoelectron Spectroscopy: A Reference Book of Standard Spectra for Identification and Interpretation of Xps Data*, pp. 40–41, Perkin-Elmer Corp., Eden Prairie, MN (1992).

47. T. Li, O. Lin, Z. Lu, L. He, and X. Wang, Preparation and characterization of silver loaded montmorillonite modified with sulfur amino acid. *Appl. Surf. Sci.* **305**, 386–395 (2014).

48. K.Y. Cho, J.Y. Moon, Y.W. Lee, K.G. Lee, J.H. Yeo, H.Y. Kweon, K.H. Kim, and C.S. Cho, Preparation of self-assembled silk sericin nanoparticles. *Int. J. Biol. Macromol.* **32**, 36–42 (2003).